

Subproject C4.1

Site-selective coupling to electrodes and transport through single molecules

Principal Investigator(s): Hilbert v. Löhneysen, Ralph Krupke, Maya Lukas

CFN financed Scientists: C. Pérez León (92.2 % BAT IIa, 30.5 months), Kerrin Dössel (75% BAT IIa, 3 months), Dirk Waibel (1/2 BAT IIa, 3 months), Cornelius Thiele (1/2 BAT IIa, 5.5 months), Tihomir Tomanic (71.4% BAT IIa, 21 months)

Further Scientists: Christoph Stroh, Marcel Mayor, Frank Hennrich, Manfred Kappes, Christoph Sürgers (people involved in the project but not financed by the CFN directly)

**Physikalisches Institut
Karlsruhe Institut für Technologie (KIT)**

**Institut für Nanotechnologie
Karlsruhe Institut für Technologie (KIT)**

Site-selective coupling to electrodes and transport through single molecules

Summary

In tailoring electrodes and molecules for functionalities in possible future molecular electronics, the controlled deposition of molecules on surfaces or to electrodes and the electronic transport and other properties of the resultant assemblies are of prime importance.

In this subproject, we investigated the deposition of and electronic transport through different molecules. Several deposition methods (dielectrophoresis in solution, sublimation in UHV, self assembly in solution, pulsed laser deposition) have been used to deposit single molecules on metal electrodes, on surfaces serving as electrodes, or in between molecular leads. Lithographically prepared electrodes, nanoscale gaps in carbon nanotubes or STM tips were used to contact the molecules. We investigated the influence of the deposition method and in particular of solvents on the bonding to the electrodes. The effect of the bonding conformation and other external effects on the transport properties have been explored.

We investigated single-walled carbon nanotubes for use as molecular leads contacting specifically tailored organic molecules. In order to form a gap in a CNT that can accommodate a single molecule, electron irradiation with the beam of a scanning electron microscope was studied. We discovered that the observed transition from the low-resistance metallic to the high-resistance insulating state by three orders of magnitude in conductance can be reversed by a large voltage bias. This cyclic process which can be repeated is attributed to charge trapped in the substrate during irradiation and mobilized by the voltage bias. With electric breakdown of a free-standing nanotube segment, gaps with a dimension < 10 nm could be formed. We succeeded in positioning an elongated chromophore molecule in the gap and were able to observe electroluminescence in a single molecule (“single-molecule flashlight”).

A major challenge in site-selective bonding of organic molecules to metal surfaces is establishing and investigating contacts with single individual molecules because elongated molecular “wires” typically used for the investigation of electronic transport properties tend to align parallel to the surface. We therefore investigated with scanning tunneling microscopy and spectroscopy a rather rigid tripodal molecule with three molecular wires (“legs”) connected to a metal-ion complex (“head”). Much to our surprise, the expected “stand-up” position was observed for less than 1% of the molecules deposited from the solution onto the Au(111) surface, while the majority of the molecules were found with two legs and the head on the Au(111) surface and the third leg protruding. This configuration allowed us to position the STM tip above different parts of the molecule, and we were able to infer from the different current-voltage characteristics the most likely path the electrons take through the molecule on their way from the tip to the metal surface. Here, density functional calculations were instrumental in determining the energies and spatial distribution of the molecule orbitals.

In a preliminary work to deposit large π -conjugated macrocycles on metal surfaces, we explored the possibility to deposit segments of these macrocycles, e.g., $C_{114}H_{158}O_8S_2Si_2$ (CHOSSI) by pulse injection with THF solvent molecules on Cu(111). We were able to image the solvent besides the CHOSSI molecules at room temperature, indicating that the solvent is immobilized by the latter and, in turn, that the CHOSSI molecules are deposited as individual species without clustering.

1. Carbon nanotubes as molecular leads

Within this subproject C4.1 carbon nanotubes (CNT) were investigated as molecular leads for contacting specifically tailored organic molecules. For this purpose we explored whether physical gaps can be formed in CNTs via exposure to a local electron beam. This first approach was not successful; however during this study a novel e-beam induced metal-to-insulator transition was observed which allows adjusting the local conductance of a CNT in a reversible manner (1.1). In the second and successful approach gaps in CNTs were formed via current-induced local oxidation. We could identify the parameter that controls the gap-size and were able to fabricate on thereby the first electroluminescing nanotube-molecule-nanotube (N-M-N) junctions (1.2). The basis for fabrication such NT-M-NT devices were advanced CNT sorting techniques provided by C3.2, the dielectrophoretic self-assembling technique [1,C4.1:4] provided by B1.9 (former C3.10), and the tailored molecules synthesized in C3.8.

1.1 Electron-irradiation induced metal-to-insulator transition

This study is related to recent developments in voltage-contrast scanning electron microscopy which allow visualizing the electronic property of carbon nanotube devices (described in B1.9) [2,3]. At low-irradiation dose this technique is non-invasive; however at large irradiation dose it has been shown that nanotube device characteristics can be altered by electron irradiation [4]. Here we wanted to induce radiation “damage” at the nanotube sidewall to form a gap of the size of the molecule to integrate.

We studied electron transport in a scanning electron microscope during repeated line-scanning across a metallic SWCNT. The most important result is the discovery of an irradiation-induced metal-to-insulator transition from a low-resistance, metallic state to a high-resistive, insulating state with a conductance difference of three orders of magnitude. Current suppression alone could have been an indication for a structural damage or gap formation. However, application of a large voltage bias leads to a transition back to the original metallic state. Moreover both states are stable in time, and transitions are fully reversible and reproducible [C4.1:8]. The insulating nanotube segment shows activated hopping conductivity, which is a characteristic of amorphous semiconductors, and is insensitive to back-gating at room temperature. We have proposed that the perturbation of the nanotube electronic system is due to charges that get trapped during irradiation in the substrate oxide underneath and can be released under voltage-bias-induced electric fields. According to our study, structural damage of the nanotube does not play a role.

Interestingly the SWCNT device is already perturbed prior to irradiation, most likely by charges that were implanted during electron beam patterning of the metal electrodes and which can also be removed by application of a large voltage. The results are of general importance to the fabrication and characterization of SWCNT devices by scanning electron microscopy.

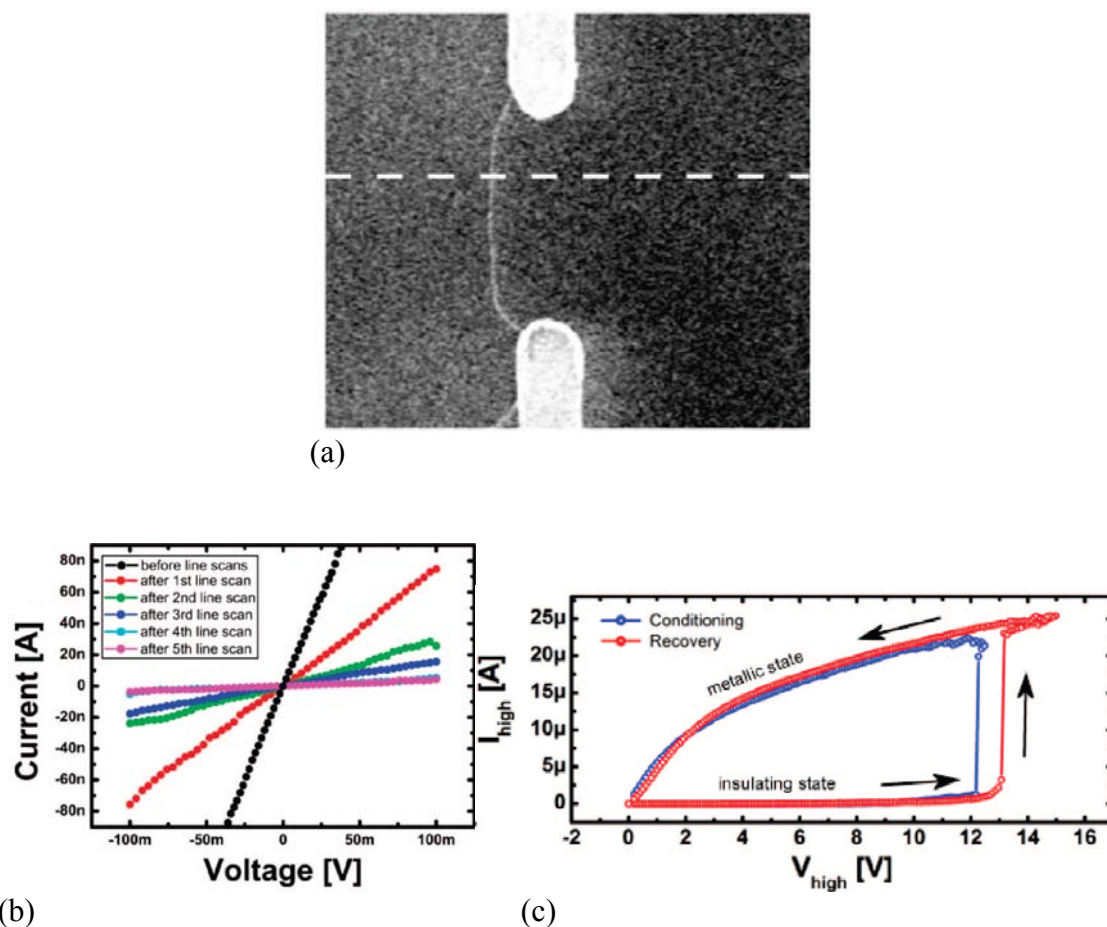


Fig.1: (a) Snap-shot scanning electron micrograph of a contacted metallic SWNT. The lateral direction and position of the electron-beam line scan is indicated by the dashed line. (b) Low-bias current-voltage characteristic of the device initially and after each line scan. (c) Reversibility of the electron-irradiation-induced transition. The arrows indicate the sweep direction of the transition from the insulating state to the metallic state. In the metallic state, the current increases linearly at low bias and shows current saturation at high bias [C4.1:8].

1.2 Electroluminescence from single nanotube-molecule-nanotube junctions

The placing of single molecules between nanoscale electrodes [5,6] has a decade long tradition and aims for their use as functional units in electronic devices. In such systems the electrical transport has been widely explored, optical measurements, however, have been restricted to the observation of electroluminescence from nanocrystals and nanoclusters [7,8], and from molecules in a scanning tunneling microscope setup [9,10]. Our motivation was to observe the electroluminescence from the core of a rod-like molecule between two metallic single walled carbon nanotube electrodes forming a rigid solid state device [C4.1:16]. The major challenge was to integrate a bottom-up object, the molecule, into a top-down structure, the CNT electrodes and to have control over the critical dimensions. Moreover the electronic and optical properties of the molecule and the carbon nanotube electrodes had to be tailored such that electron transport and light emission is possible. Along these considerations, the fluorescent molecule displayed in Fig. 2a was designed in C3.8 [C4.1:17]. Its rod-like structure with a length of 6.6 nm between two terminal phenanthrene units (green in Fig. 2a) should enable to bridge a nanometer-sized gap in a single-walled carbon nanotube. It

consists of a central 2,6-dibenzylamino core-substituted naphthalenediimide (NDI) dye (blue in Fig. 2a), which is known to have a strong fluorescence signal in the red. The chromophore is functionalized symmetrically with two long oligo(phenylene ethynylene) (OPE) rods (red in Fig. 2a) as polarizable π -systems along the molecule's axis to allow for electrostatic trapping in the nanotube gap. These OPE rods bear terminal phenanthrene units as flat π systems to favor their attractive interaction with the nanotube ends of the junction.

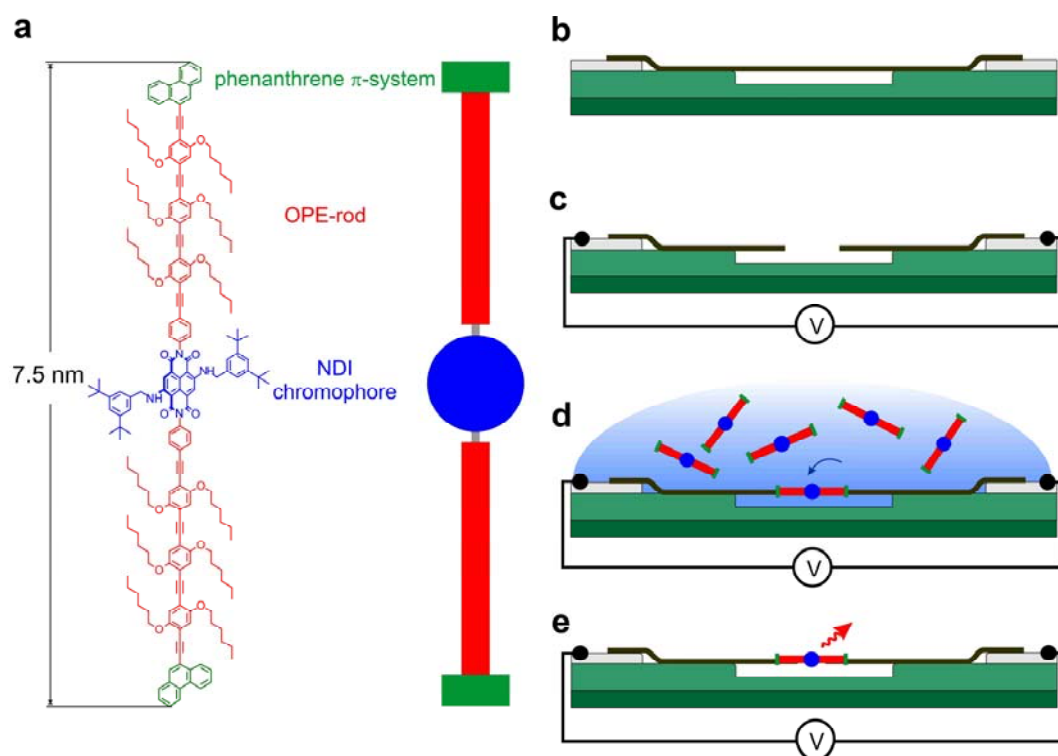


Fig. 2 (a) Structure of the molecule, consisting of a central 2,6-dibenzylamino core-substituted NDI chromophore (blue), two OPE rods (red), and phenanthrene anchor units (green). (b-e) Schematics of the device fabrication. (b) After dielectrophoretic deposition, a metallic nanotube (black) bridges Pd electrodes (gray), and is free-standing above a trench in silicon oxide (green). (c) Electrical breakdown opens a gap in the nanotube. (d) Dielectrophoretic deposition of the polarizable molecule from solution into the nanotube gap leads to the formation of a NT-M-NT junction. e, Light emission from the molecule under voltage bias V is detected and analyzed in an optical-microscope setup (not shown).

Briefly, we have started by assembling metallic nanotube devices by the dielectrophoresis method (Fig. 2b) and obtained low ohmic device characteristics by high current conditioning. Nanogaps were formed in the free standing nanotube segment above a trench (Fig. 2c and Fig. 3a) by electric breakdown. The gap size was controlled by the oxygen partial pressure and yielded below 10 nm for 50% of the gaps prepared under high vacuum. The molecules were translocated by dc dielectrophoresis and trapped into the biased nanotube nanogaps from solution.

The electroluminescence experiments were performed in vacuum to avoid quenching of the excited state by oxygen. Fig. 3b shows the integrated electroluminescence (EL) signal of a NT-M-NT contact at $V = 4$ V, measured in reflection mode with an acquisition time of $t = 20$ min. The EL can be switched on and off with V . To locate the emission, an image recorded under external illumination is overlaid. A bright spot is clearly seen between the electrodes of the biased device.

Similar emission spots have been observed for 6 out of 20 biased NT M NT contacts. We succeeded in measuring the EL spectrum of the contact of Fig. 3b, with $t = 60$ min, $V = 5$ V and $I = 20$ nA, as shown in Fig. 3c. We observe a peak of the EL at $\lambda_{\text{EL}} = 680$ nm with a full width at half maximum (FWHM) of ~ 85 nm, and a small shoulder in the near infrared. The EL spectra is very similar in terms of peak position, width and overall spectral shape to the fluorescence (FL) spectrum of the molecule on HOPG. This spectroscopic fingerprint of the molecule is evidence for molecular electroluminescence.

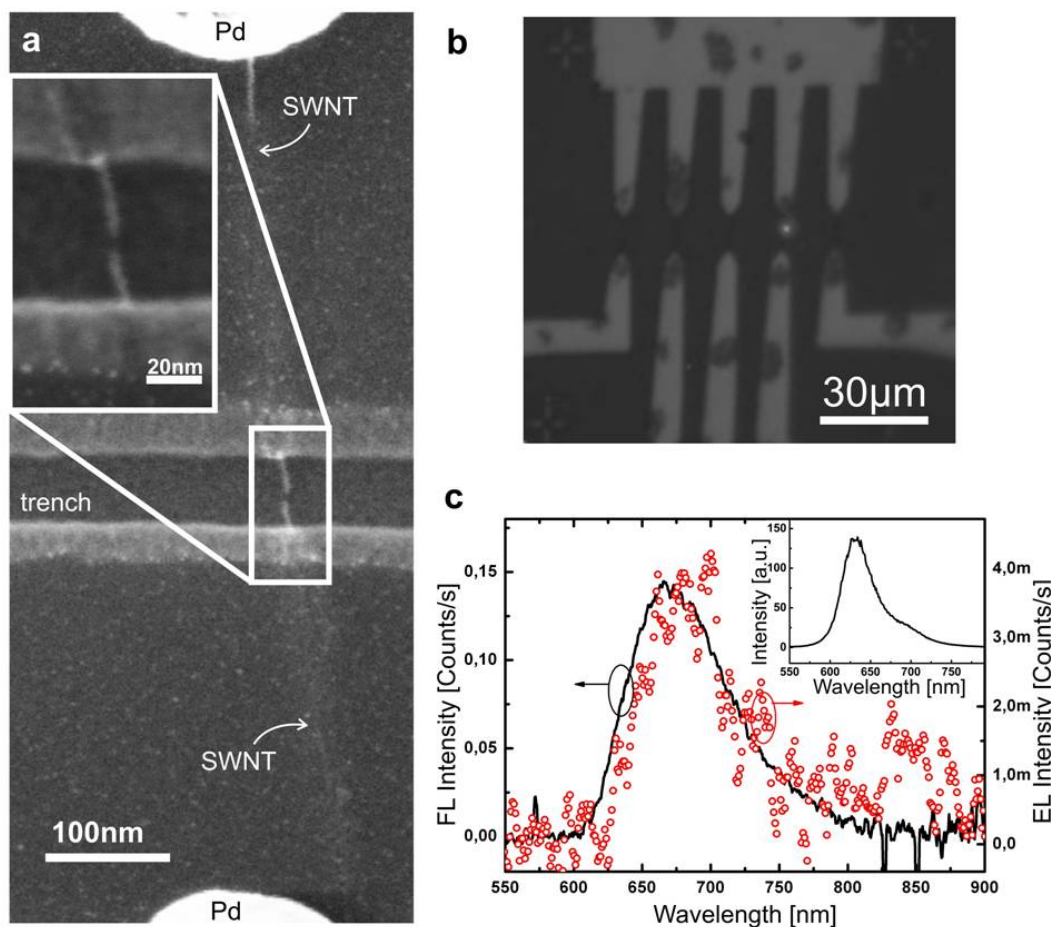


Fig 3 (a), Scanning electron micrograph of a contacted metallic nanotube after electrical breakdown under high vacuum (HV), corresponding to Fig. 1c. The nanotube connects the Pd electrodes and exhibits a gap of approximately 7 nm width in its free-standing segment above the SiO₂ trench. The substrate supported nanotube segments are barely visible compared to the free standing segments, due to voltage contrast effects. Gap region is shown in the inset. (b), Optical micrograph recorded under external illumination shows five device structures with Pd source and drain electrodes, bridged by NT M NT junctions (not visible). Overlaid is an image acquired for 20 min without external illumination. (c), EL spectrum of the NT M NT junction shown in b, integrated for 60 min at $V = 5$ V and $I = 20$ nA (\circ). The data is compared with the FL spectrum of molecules on highly oriented pyrolytic graphite (M/HOPG) (black line). Both spectra show a close similarity.

2. Site-selective bonding and electronic transport through tripodal molecules

Electronic transport properties of organic molecules have been investigated within the CFN by mechanically controlled break junction (MCBJ) experiments in the first funding period [11]. As a result of these and other investigations it was found that the molecule-electrode bond, the conformation of the molecule and its surroundings play a crucial role in the conductance [12]. In contrast to the MCBJ method, it is possible to directly address single atoms or molecules on a conducting surface by scanning tunneling microscopy (STM) and spectroscopy (STS) [13]. This method is therefore capable of characterizing single molecules prior to the actual conductance measurement, e.g. to investigate the molecular conformation, the bonding position on the surface and possible intermolecular interactions [C4.1:14, C4.1:9]. Elongated molecular “wires” that are typically used for investigation of electronic transport properties tend to bind with their long axis parallel to the surface electrode. Therefore, for electronic transport measurements they are usually brought into an upright position by self-assembled monolayers or by picking them up by an STM tip [12]. Picking up one side of the molecules with the STM tip will alter the bottom bond and very likely also the conformation of the molecule and both could differ from one conductance measurement to the other. In order to circumvent this problem, a rather rigid three-dimensional molecule has been synthesized. Three identical molecular wires (legs) are connected by a metallic complex (head) to form a tripodal structure. The legs end in a foot group which might be altered to vary the interaction with the surface. [14] All rotations around bonds that are possible within the molecule conserve the three-dimensional structure. Regardless of the molecule’s bonding configuration, either the head or at least one of the three legs will protrude from the surface being accessible by the STM tip.

2.1 Site-selective bonding of tripodal molecules

A molecule with a Ga III complex as a head group and SCH₃ feet was synthesized (see Fig. 5 a). The molecules were first sublimated in UHV onto in-situ cleaned Au(111) crystals. This approach did not lead to reproducible results, probably because molecules do not stay intact during the sublimation and deposition process. Hence we turned to deposition from solution: The Au(111) single crystal surface was cleaned *in situ* and transferred to the load lock of the UHV system. A droplet of solution ($V \approx 8 \mu\text{l}$, $c \approx 2 \cdot 10^{-6} \text{ mol/l}$) was deposited onto the clean surface in the opened load lock, while a steady flow of N₂ was maintained to prevent contamination from air. The load lock was then closed and pumped immediately.

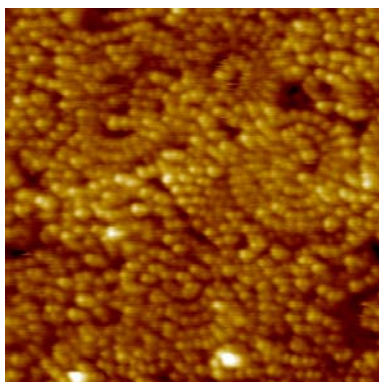


Fig. 4: CH₂Cl₂ on Au(111) forms dimer-strands that arrange in double rows and rosette structures.

The solvent, CH_2Cl_2 , is highly volatile and a drop evaporates from the surface within seconds. Nevertheless a monolayer of CH_2Cl_2 molecules can be found to remain on the surface (Fig. 4). The polar molecules order in double-strand structures with at least medium-range order, which can be explained by their dipolar character.

Fig. 5b shows a typical sample with a submonolayer of molecules deposited from solution onto a Au(111) surface. Remaining solvent (seen as bright areas in the middle and lower right area of the image) can be removed by annealing the sample to $T=323\text{K}$ for 10 minutes, while the number of molecules does not decrease noticeably.

Although the interaction of the molecules with the surface is weak, as indicated by the persistence of the herringbone reconstruction [15] up to rather high coverages, the position of the molecules is stable during imaging by STM at 30K. We see a distinct influence of the surface-molecule interaction on the bonding position of the molecules. Molecules preferably bind at the elbows and in the fcc regions of the reconstruction while hcp regions are less covered. The transition regions are not covered at all at low coverage. This preferential binding to special regions of the surface might be due to electronic reasons [16] or due to strain related energetics. [17]

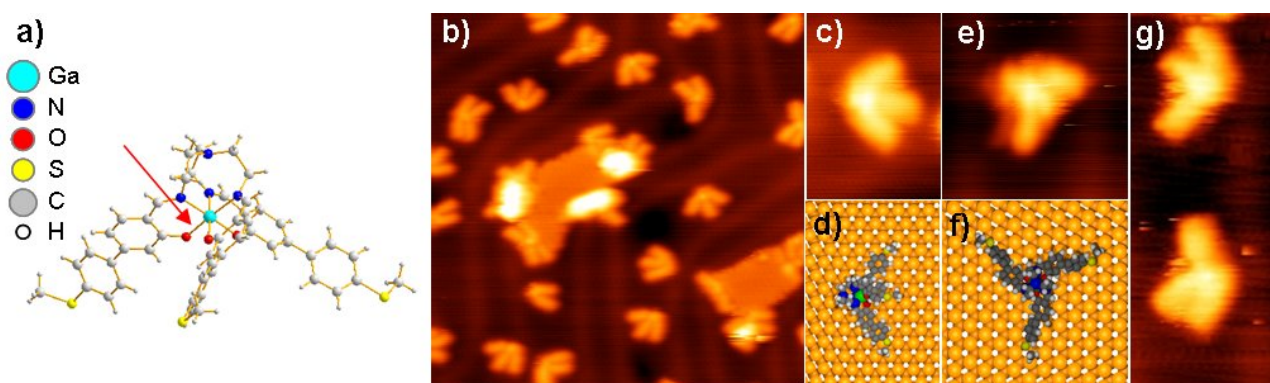


Fig. 5 (a) Structure of the molecule as found by x-ray diffraction. (b) Submonolayer of the molecules on Au(111). The two bright areas are remaining solvent which can be removed by annealing. Several conformations can be found: (c) STM image and (d) schematic picture of a molecule in „duck’s foot“ conformation. (e) STM image and (f) schematic picture of a standing molecule. (g) STM image of two molecules with broken head-bond.

There is no substantial interaction between the molecules on the surface: they are never forming ordered layers even at the highest coverage.

The conformation of intact molecules that is mainly found (ca. 40%) on the Au(111) surface is shown in Fig. 5c. It can be assigned to a molecule with two legs and the head on the surface and the third leg protruding, as schematically shown in Fig. 5d. A very small fraction of molecules ($< 1\%$) is standing in a lunar module orientation as shown in Fig. 5e, f. A significant number of molecules is found in a configuration which cannot be identified by any orientation of an intact molecule on the surface. The weakest bond in the molecule is the bond of the leg to the head marked by arrow in Fig. 5a. Breaking of this bond allows for a rotation of the leg around the remaining bond. This leads to a configuration of the molecule which resembles the shape seen in Fig. 5g.

The observation, that a substantial part of the molecules is not intact anymore after deposition is of great importance. A molecule which is found to be stable in “conventional” dilution as used for the chemical analysis might become unstable in the same solvent at very high dilutions. These high dilutions are frequently used when aiming for submonolayer coverage, as is the case in single-molecule conductance measurements. Another possibility is that the surface acts as a bond-breaking

catalyst for the molecule in solution. In both cases contacting the alleged molecule by a “blind” method as MCBJ will be useless to gain insight into fundamental molecular conduction processes, because a substantial part of contacts will comprise defective molecules. This emphasizes the importance of characterizing the molecule-electrode contact.

Deposition on highly oriented pyrolytic graphite (HOPG) and Ag(111) did not lead to stable and reproducible results.

2.2 Electronic transport through tripodal molecules

To gain insight into the electronic properties of the molecule $I(V)$ measurements were performed on the molecule in the conformation of Fig 5c [18]. The tip was positioned above well defined locations above the molecule, the position was fixed and the voltage ramped from $V=0$ to positive or negative voltage while the current was monitored. In recent years several methods have been proposed to extract the DOS from $I(V)$ measurements. Here we follow the approach of Wagner et al. [wagner], which also allows for averaging over measurements at different current and voltage setpoints, i.e. sample-tip distances.

Fig. 6 shows the DOS deconvolved from the measurements above the head or the legs of the molecule. We also distinguished between the protruding middle leg and the side legs. The differences between spectra measured above the head and above the side legs are striking: The spectra seem to be almost anticorrelated. A clear maximum in the spectra at one position corresponds to a minimum in the respective other position ($V = -2.7, -2, -1.3, +2.7V$). It is obvious that these spectra reflect the energetical but also the local variation of molecular orbitals. Depending on the path of electrons through the molecule we expect to find signature of the DOS of the traversed sections in the spectrum. The “anticorrelation” of spectra on head and side legs indicates that orbitals are either located at the head or the leg at the respective energies and furthermore a complete lack of electron transport between the side legs and the head. Instead electrons tunnel directly from the surface through the respective section into the tip (or vice versa). On the contrary in spectra on the middleleg we find all of these peaks, which indicates transport between the head and the leg, that is lifted from the surface.

We performed density functional theory (DFT) calculations of the molecule in gas phase to test our interpretation. The calculated molecular orbital energies are added to the spectra as grey bars. The chemical potential was placed halfway between HOMO and LUMO and all orbital energies were shifted by a fixed $\Delta E = 0.3eV$ to best match the peaks in the measured spectra. The surprisingly good overall match of the calculated DOS with the main features of the spectra indicates once more the weak interaction between molecule and surface.

The spatial extend of the respective calculated orbitals is shown in Fig. 6 in the small insets labelled a-j. The location of the calculated orbitals agrees very well with the local variations found in the measured spectra. E.g. the orbitals b and h are located at the legs and accordingly spectra on the side legs show a maximum while spectra above the head show a minimum at the respective energies. Orbital e is the only case where the calculated location of the orbital does not fit the local spectra. Since the orbitals are spread over the whole molecule we would expect not only maxima when measuring above the legs but also when above the head. We assume an energetic shift for the orbital located at the head due to an interaction the gold surface state that is locally and energetically close (at $-0.5V$). Orbital d is located at the head, accordingly we measure a maximum

above the head and a minimum above the side leg at this energy. On the contrary for spectra measured above the protruding leg, we find a maximum as well. In this case electrons are tunneling from the surface into the head orbitals and from there fading into the protruding leg and tunneling to the tip.

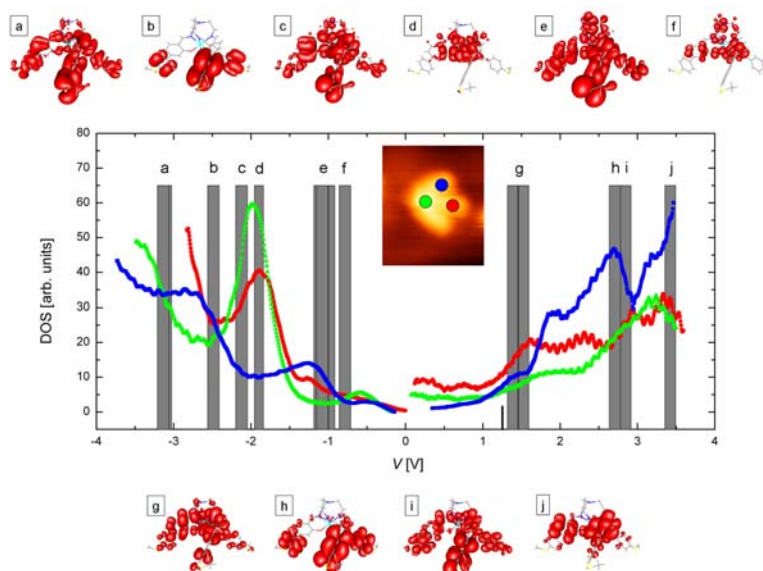


Fig. 6: Locally resolved spectroscopy on the tripodal molecule (curves) and calculated orbital energies (grey bars). The local extent of the respective orbitals is indicated in the small images a-j for occupied and unoccupied orbitals above and below the spectra respectively.

We therefore observe to different paths of electrons through the molecule. With the leg protruding, electrons rather tunnel through the head and along the leg to the tip. If the leg is not protruding and thus interacting with the surface, electrons are rather tunneling directly across the leg into the tip. We emphasize that all legs are connected to the head by the same bonds and that the difference in conductance is solely due to the different coupling of the legs to the surface. We thus observe different conduction paths in dependence of the orientation and coupling of a molecular wire to the surface.

2.3. Outlook

Two further molecules, one with a different foot group and one with a different head complex have successfully been synthesized and are currently under investigation. We find pronounced differences in the assembly as compared to the Ga III tripod. The analysis of the findings, some concluding measurements and the synthesis and STM investigation of a molecule without binding foot-group are object of ongoing work.

3. Codeposition of large π -conjugated oligomers and tetrahydrofuran on Cu (111)

The common method for depositing organic molecules under UHV conditions is by thermal sublimation. This method, however, can neither be applied to reactive molecules nor to large molecules. Because molecules of high molecular weight need a very high temperature to be evaporated it is often more likely that they are finally fragmented or degraded due to pyrolytic

decomposition. A very promising method to deposit large macrocycles such as $C_{768}H_{928}O_{64}S_{16}$ [19] is the so-called “pulse-injection” [20], where a solution of the target molecules is injected into the UHV chamber using a high-speed solenoid pulse valve. This approach has the advantage compared with solution-based deposition methods that the substrate is never exposed to air throughout the preparation, so that the sample is prepared *in situ*.

In the present work, the deposition of π -conjugated organic oligomer $C_{114}H_{158}O_8S_2Si_2$ (CHOSSi) dissolved in tetrahydrofuran (THF) by pulse injection on Cu(111) was investigated by STM at room temperature [C4.1:12]. Fig. 7 shows the CHOSSi molecule (molecular weight: 1776.77) which corresponds to a piece of the giant macrocycle $C_{768}H_{928}O_{64}S_{16}$ (CHOS) [19]. The CHOS macromolecule has a diameter of about 12 nm and consists of conjugation-active subunits, such as acetylene- and diacetyleneconnected para-thiophene and para-benzene rings. In a first approach, we have studied the deposition and adsorption of the CHOSSi oligomer on the clean Cu(111) surface by STM in UHV at room temperature.

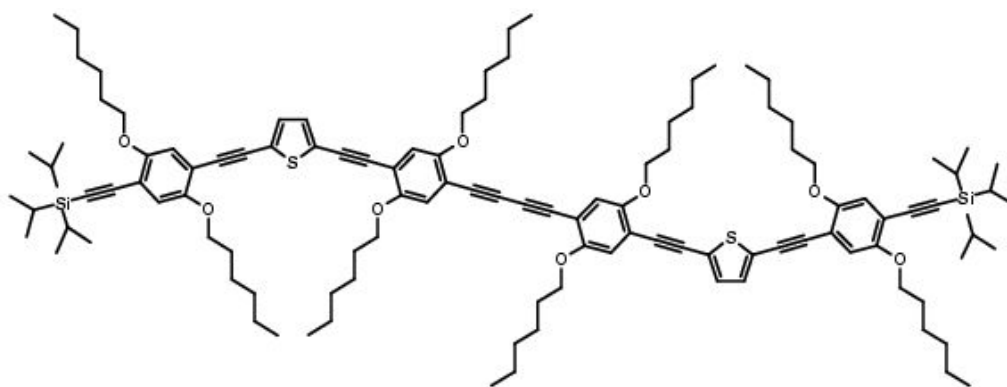


Fig. 7: The $C_{114}H_{158}O_8S_2Si_2$ (CHOSSi) molecule.

The investigated CHOSSi oligomer was synthesized as described previously [19]. The silicon moieties $Si-(CH)_3(CH_3)_6$ act as protector groups at the ends of the molecule, and separate when dissolving the oligomer in THF (tetrahydrofuran anhydrous, 99.9%, inhibitor-free). The target solutions were prepared by dissolving 0.14 mg of CHOSSi in 10 ml of THF, to obtain a concentration $\sim 8 \times 10^{-6}$ M. The Cu(111) substrate was cleaned by several cycles of 1 – 2 keV Ar^+ sputtering and subsequent heating up to 550 °C. Terraces of several tens of nanometers could be identified with the STM and the cleanliness of the surface was confirmed by Auger electron spectroscopy. The base pressure in the deposition chamber was lower than 2×10^{-9} mbar. For the deposition of molecules the sample was placed in a horizontal position 10 cm below the nozzle of the pulse valve. The valve was opened for a short time of 10 to 12 ms, once or several times. During the opening of the valve the pressure increased to $1 - 4 \times 10^{-6}$ mbar and recovered within a few minutes. Afterwards, the sample was transferred to the analysis chamber where the base pressure was lower than 1×10^{-10} mbar. The amount of CHOSSi molecules, solvent and impurities that reach the substrate can be estimated from the intensities of the C, O, S, Si, and Cu lines of the AES spectra. The sample was subsequently imaged by STM using cleaned W and Pt/Ir tips.

Fig. 8 shows images of the clean Cu(111) surface before deposition (a) and after deposition of CHOSSi and THF (b–e). Images b–e show several bright protrusions of different sizes which can be distinguished from an ordered background. The measured features can be classified by taking into account their geometry and apparent size. Spots of about 4 nm diameter are ascribed to single

CHOSSi molecules. In Fig. 8c,e some individual oligomers are marked with a circle. These molecules appear to be distributed randomly on the surface. The oligomers are surrounded by other structures. Somewhat smaller features (about 2–2.5 nm size) presumably correspond to the $\text{Si}(\text{CH}_3)_3(\text{CH}_3)_6$ groups remaining in the solution during the deposition, which separate from the CHOSSi oligomer when dissolved in THF. These silicon moieties show 2 or 3 lobes corresponding to their orientation with respect to the surface, see arrows in Figs. 8c,e. The origin of the ordered background is currently investigated in detail. Additional solvent molecules are adsorbed on this layer appearing as small isolated dots of 0.6 to 1 nm in Fig. 8b,c,e. Other features appearing in the STM measurements are expected to be molecular clusters or impurities.

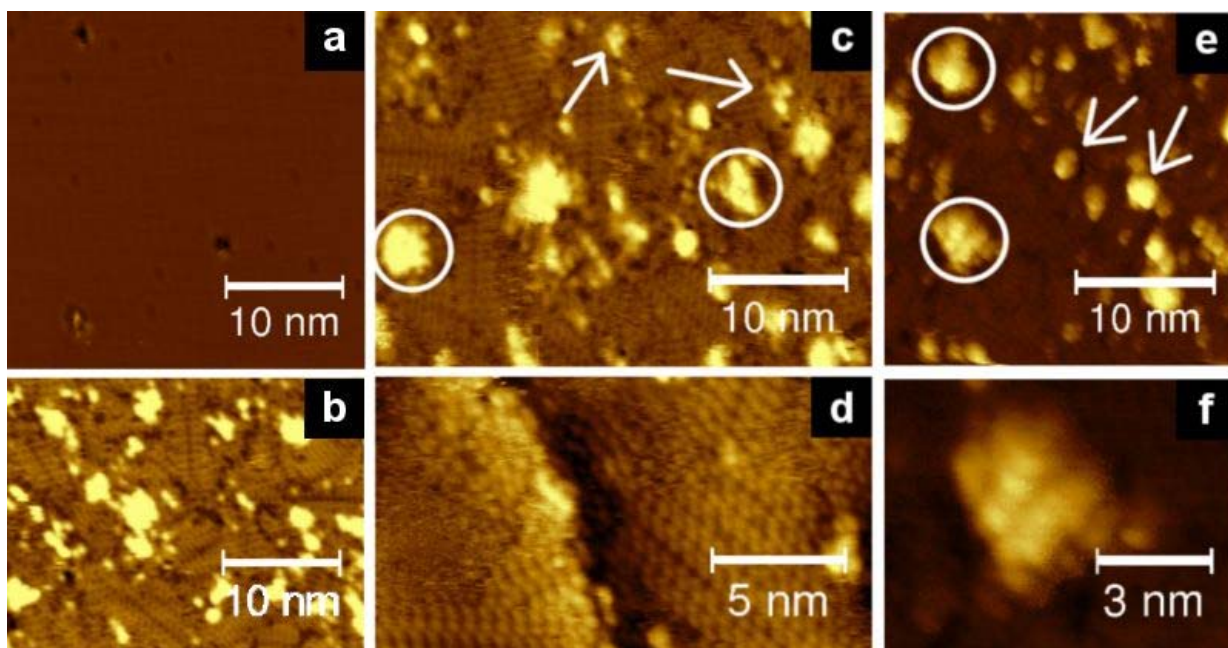


Fig. 8: STM images taken at room temperature. (a) Cu(111) before deposition; image size $35 \times 35 \text{ nm}^2$ (tunneling current 0.70 nA, tunneling bias 0.9 V). (b–e) Cu(111) after deposition of CHOSSi and THF. (b) $40 \times 31 \text{ nm}^2$; 0.20 nA, 2.5 V. (c) $35 \times 25 \text{ nm}^2$; 0.70 nA, 2 V. (d) Self-organized domains, $18 \times 10 \text{ nm}^2$; 20 nA, 2.5 V. (e) $25 \times 25 \text{ nm}^2$; 0.20 nA, 2 V. (f) Image of a single CHOSSi molecule, $10 \times 8 \text{ nm}^2$; 0.20 nA, 2 V. Circles indicate individual CHOSSi molecules. Arrows indicate individual $\text{Si}(\text{CH}_3)_3(\text{CH}_3)_6$ groups.

Figure 8f shows an image of a single CHOSSi molecule with higher resolution. It is worth noticing that the appearance of the individual oligomers changes from one position to another (Fig. 8b,c,e). This effect is probably due to different adsorption configurations of the molecules on the Cu(111). The configuration geometry results from the substrate-molecule interaction, but is also strongly influenced by the solvent and the deposition technique.

Although the pulse-injection method is a reliable deposition technique for large molecules the influence of the solvent on this process is still not well understood. Our previous tests performed with CHOSSi molecules dissolved in chloroform were not successful. Thus, the presence of the THF solvent seems to play an important role in the adsorption of the oligomers on the copper surface. The coadsorption of the solvent with the CHOSSi molecules probably prevents the

CHOSSi oligomers from aggregation, allowing their deposition as individual species. Furthermore, it provides a matrix where the molecules are embedded avoiding their migration over the surface of the substrate during the scan, thereby permitting their imaging by STM. The formation of larger domains of the self-ordered structures in Figs. 8b-d is probably prevented by the coadsorption of the CHOSSi oligomers. The orientation of the different domains appears to follow selected directions that can be associated with the orientation of the (111) plane of copper, see Fig. 8b,c.

The fact that the solvent could be imaged at room temperature coadsorbed with the target molecules indicates a very strong interaction of the THF molecules with the substrate. The codeposition of solvent molecules with the target ones has been proposed by several groups who used the pulse-injection deposition method. However, these investigations were done at low temperatures. To date, no reports of the observation of the pulse-injection codeposited solvent molecules at room temperature have been published. The main argument is that small molecules can migrate rapidly at room temperature not allowing to be imaged. Toluene and methylene chloride coadsorbed with an organometallic molecule onto Au (111) at 77 K [21]. In that case stripes with multiple orientations on the Au(111) surface were observed, similar to the present case, suggesting that the preferred orientation is due to the interaction with the underlying surface.

In summary, the codeposition of π -conjugated oligomers (CHOSSi) and THF-solvent molecules on Cu(111) with the pulse-injection method has been characterized with STM at room temperature. To our knowledge, this is the first time, that a solvent has been pulse-deposited and imaged coadsorbed with the target molecules at room temperature. We mention that the deposited molecules show a dependency of the tunneling parameters, showing different electronic states for the distinct species. The present results serve as an important prerequisite for the deposition of the large $C_{768}H_{928}O_{64}S_{16}$ macrocycles, dissolved in THF, by pulse injection.

References

Own publications originating from the scientific work performed in this subproject are cited with full title.

- [1] A. Vijayaraghavan, F. Hennrich, N. Stürzl, M. Engel, M. Ganzhorn, M. Oron-Carl, C.W. Marquardt, S. Dehm, S. Lebdkin, M.M. Kappes, R. Krupke, *Single-Chirality Carbon Nanotube Device Arrays*, ACS Nano **4**, 2748 (2010)
- [2] A. Vijayaraghavan, S. Blatt, C. W. Marquardt, S. Dehm, R. Wahi, F. Hennrich, R. Krupke, *Imaging electronic structure of carbon nanotubes by voltage-contrast scanning electron microscopy*, Nano Research **1**, 321 (2008)
- [3] A. Vijayaraghavan, C.M. Marquardt, S. Dehm, F. Hennrich, R. Krupke, *Defect Imaging in Single-Walled Carbon Nanotubes by Voltage-Contrast Scanning Electron Microscopy*, Carbon **48**, 494 (2010)
- [4] A. Vijayaraghavan, K. Kanzaki, S. Suzuki, Y. Kobayashi, H. Inokawa, Y. Ono, S. Kar, P.M. Ajayan, Nano Lett. **5**, 1575 (2005)
- [5] M.A. Reed, C. Zhou, C.J. Muller, T.P. Burgin, J.M. Tour, Science **278**, 252 (1997)
- [6] Reichert, J. et al., Phys. Rev. Lett. **88**, 176804 (2002)

- [7] J.I. Gonzalez, T.-H. Lee, M.D. Barnes, Y. Antoku, R.M. Dickson, *Phys. Rev. Lett.* **93**, 147402 (2004)
- [8] M.S. Gudixsen, K.N. Maher, L. Ouyang, H. Park, *Nano Lett.* **5**, 2257 (2005)
- [9] X.H. Qiu, G.V. Nazin, W. Ho, *Science* **299**, 542 (2003)
- [10] Z. Dong, et al., *Phys. Rev. Lett.* **92**, 086801 (2004)
- [11] M. Mayor, H. B. Weber, J. Reichert, M. Elbing, C. von Hänisch, D. Beckmann, and M. Fischer, *Electric Current through a Molecular Rod-Relevance of the Position of the Anchor Groups*, *Angew. Chem. Int. Ed.* **42**, 5834–5838 (2003)
- [12] C. Li, I. Pobelov, T. Wandlowski, A. Bagrets, A. Arnold, and F. Evers, *J. Am. Chem. Soc.* **130** (1), 318-326 (2008)
- [13] M. Schöck, C. Sürgers, and H. v. Löhneysen, *Atomically resolved tunneling spectroscopy on Si(557)-Au*, *Europhys. Lett.* **74** (3), 473-478 (2006)
- [14] C. Stroh, in preparation
- [15] C. Wöll, S. Chiang, R. J. Wilson, and P. H. Lippel, *Phys. Rev.* **B 39**, 7988 (1989)
- [16] L. Bürgi, H. Brune, and K. Kern, *Phys. Rev. Lett.* **89**, 176801 (2002)
- [17] P. Maksymovych, O. Voznyy, D. B. Dougherty, D. C. Sorescu, J. T. Yates Jr., *Prog. Surf. Sci.* **85**, 206 (2010)
- [18] K. Dössel, M. Lukas, A. Schramm, K. Fink, O. Fuhr, C. Stroh, M. Mayor, and H. v. Löhneysen, *Tracking the path of electrons through a multiterminal molecule*, submitted for publication
- [19] M. Mayor, C. Didschies, *A Giant Conjugated Molecular Ring*, *Angew. Chemie Int. Ed.* **42**, 3176 (2003)
- [20] H. Tanaka, T. Kawai, *J. Vac. Sci. Tech. B* **15**, 602 (1997)
- [21] S. Guo, S. A. Kandel, *J. Chem. Phys.* **128**, 01470 (2008)